Jpn. J. Appl. Phys. Vol. 42 (2003) pp. 1395–1399
Part 1, No. 3, March 2003

X-Ray Reflectivity Study of Interdiffusion at $YBa_2Cu_3O_{7-x}$ and Metal Interfaces

S.-W. HAN[1]*, S. TRIPATHY[1], P. F. MICELI[1], E. BADICA[2], M. COVINGTON[2], L. H. GREENE[2] and M. APRILI[3]

[1]*Department of Physics and Astronomy, University of Missouri-Columbia, Columbia, Missouri 65211, U.S.A.*
[2]*Department of Physics, University of Illinois at Champaign-Urbana, Urbana, Illinois 61801, U.S.A.*
[3]*CSNSM-CNRS Bat. 108 Universite Paris-Sud, 91405 Orsay, France*

(Received August 13, 2002; accepted for publication September 26, 2002)

We present a study of interdiffusion at interfaces of $YBa_2Cu_3O_{7-x}$ (YBCO) and metals, Au, Ag, and Pb by using X-ray reflectivity. YBCO thin films were epitaxially grown by off-axis sputter deposition and coevaporation, with the *c*-axis perpendicular to the $SrTiO_3$ substrate surfaces. The capping layers were subsequently deposited on the YBCO film *in situ* and *ex situ* near room temperature. Glancing incident X-ray reflectivity was employed to investigate the surfaces and their buried interfaces. We find that interdiffusion at the interfaces of Au/YBCO and Ag/YBCO is negligible. However, a large interdiffusion zone, ~60 Å, is present at the Pb/YBCO interface and the lead films grown, both *in situ* and *ex situ*, were entirely oxidized. We do not observe any diffraction peaks from the Pb/YBCO films. The diffraction peaks are found up to (007) from the YBCO films of the Au/YBCO and Ag/YBCO films. This implies that the loss of crystalline structure in a ~300-Å-thick YBCO film underneath Pb is caused by interdiffusion. [DOI: 10.1143/JJAP.42.1395]

KEYWORDS: interdiffusion, interface, surface, thin film, reflectivity, X-ray, YBCO, superconductor

1. Introduction

$YBa_2Cu_3O_{7-x}$ (YBCO) has attracted considerable attention for its high superconducting transition temperature ($T_c \simeq 90$ K) and high critical current density.[1,2] These properties of a superconductor are very important for practical applications. For studies of Josephson junction tunneling, proximity effect and other applications, the interfaces of Pb/YBCO,[3–12] Au/YBCO[13–15] and Ag/YBCO[16,17] have been widely used. Also it is known that a small amount of silver[18–20] or gold[21,22] doping does not affect T_c but precipitates to grain boundaries where it enhances the YBCO grain (twin domain) size. Thus, it is worth studying interdiffusion at the interfaces of YBCO and metals. Several techniques have been employed for understanding the Au/YBCO and Ag/YBCO interfaces, including transmission electron microscopy (TEM),[23,24] resistivity[25] and microwave surface resistance[26] measurements. These studies showed that the interfaces of Au/YBCO and Ag/YBCO are electronically well-contacted. However, TEM imaging can show only a small portion of the cross section of the interfaces after cutting the sample and resistivity measurements can not measure interface morphology. Furthermore, little is known about the Pb/YBCO interface, although there is an ongoing debate in the subject of Josephson tunneling through a Pb/YBCO tunnel junction regarding whether the pairing symmetry is s-wave or d-wave.[7–12]

We performed glancing incident X-ray reflectivity (GIXR) measurements at the YBCO and metal interfaces. To our knowledge, GIXR studies of interdiffusion at the YBCO metal interfaces have never been made. Previous GIXR studies have been quite successful in understanding the surfaces of YBCO films,[27–29] though a thick YBCO film is problematic in GIXR studies because of anomalous diffuse scattering which suppresses the specular reflectivity, particularly, just above critical angle due to a large disordered zone at the air/YBCO interface. The schematic geometry of GIXR is shown in inset of Fig. 1. The

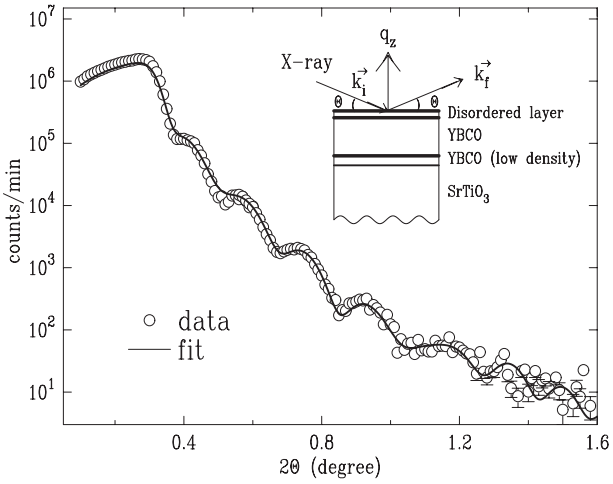

Fig. 1. X-ray from a YBCO/$SrTiO_3$ sample as a function of 2θ. The solid curve is a best fit. The inset shows X-ray reflectivity geometry where $\vec{k}_i$ and $\vec{k}_f$ are incident and exiting X-ray wave vectors with angle θ and q_z is momentum transfer. The YBCO layers, which have different X-ray scattering density, are also shown in the inset.

reflectivity from a rough surface can be written as,[30–32]

$$R = R_0 e^{-q_z^2\sigma^2/2}, \tag{1}$$

where R_0 is reflectivity[33] from a smooth surface, σ is rms roughness and q_z is momentum transfer, $4\pi \sin\theta/\lambda$ with θ being the X-ray incident angle and λ the incident X-ray wavelength. A disordered zone at an interface contributes to the σ in the reflectivity in addition to the roughness. It means that the roughness and interfacial disorder can not be independently determined from a single GIXR measurement. Therefore, we should know the surface roughness first without a capping layer because the interdiffusion can be determined only by comparing the reflectivities from the same specimen with and without the capping layer. However, YBCO is problematic because the surface is considerably sensitive to air. As the capping layer is deposited on the YBCO after GIXR measurement from a naked YBCO film, the GIXR measurements may not provide correct information of the interdiffusion because the YBCO surface would

*Present address: Chemical Sciences Division, Lawrence Berkeley National Laboratory, Berkeley, California 94720, U.S.A.

be changed during the measurements and transportation in air. There were a number of actions we could have taken to avoid this problem, such as, *in situ* GIXR measurements and *in situ* coating of the YBCO surface with a material which does not react with YBCO. We chose the latter method because it requires less cost. We prepared two YBCO films which were adjacently deposited on each $SrTiO_3$ substrate, one of the YBCO films was covered by a mask *in situ* and the other one was subsequently metalized with gold. We believe that the surfaces of the two YBCO films are similar before the gold layer was coated. From GIXR, we found that there is an extra layer with low scattering density developed on the naked YBCO surface whereas the interface of Au/YBCO remains clean. We concluded that the interdiffusion at the Au/YBCO is negligible and used the YBCO surface underneath the gold film as a standard to discern whether the interdiffusion is present at the interfaces of YBCO and the other metals.

In §2, we discuss the experimental details of the preparation of YBCO, Au/YBCO, Ag/YBCO and Pb/YBCO samples, and GIXR measurements from the samples. The analysis of the GIXR data and results are presented in §3. We discuss the results in §4 and summarize the main conclusions in §5.

2. Experiment

Five thin YBCO films with thickness $\sim$300 Å were prepared for the interdiffusion study. Each YBCO film was epitaxially grown on $SrTiO_3$[001] substrates with the resultant *c*-axis perpendicular to the substrate surface. Two YBCO films were simultaneously sputtered[34] on each substrate in total pressure 110 mTorr of argon and oxygen in the ratio $Ar : O_2 = 5 : 1$ with the substrates temperature held at 720°C. These parameters were optimized to obtain a smooth surface. After sputtering the YBCO layer, one of the YBCO thin films was covered with a stainless steel mask *in situ* and the Au (300 Å) layer was successively sputtered on the other film, in 7 mTorr Ar only. The substrate temperature was held at 65°C during this part of the sputtering process. For the Pb deposition, a YBCO (300 Å) film was deposited by the sputter with the same conditions as the YBCO film mentioned above, the film was quickly ($\sim$2 min) moved to another chamber in air, and a Pb (300 Å) film was evaporated on the YBCO film at room temperature.[3–5] The resistivity of the 300-Å-thick YBCO film at room temperature was 294 μΩcm. The Ag(300 Å)/YBCO(300 Å) and Pb(300 Å)/YBCO(300 Å) films were deposited by a coevaporation technique,[6] i.e., Y, Ba and Cu are evaporated separately in an atmosphere of atomic oxygen. The YBCO stoichiometry 1 : 2 : 3 was accurately controlled within an uncertainty 1–2%. During the growth of YBCO, the substrate temperature was held at 750°C and the oxygen partial pressure was $\sim$1 mTorr. After the YBCO was deposited, the O_2 partial pressure was increased up to 700 mTorr and the substrate was cooled down to room temperature. Then, the chamber was pumped to 10^{-8} Torr and the Ag or Pb was evaporated *in situ* on the YBCO fresh surface. The T_c of a similar sample was 86 K and the resistivity was 150 μΩcm at room temperature.

X-ray reflectivity measurements were carried out in air at room temperature. We used a line beam X-ray (width $\sim$0.15 mm at sample position) with wave length 0.70926 Å, Mo $K\alpha_1$, which radiates from a rotating Mo anode and reflects from a Ge(111) monochromater. The distance of the X-ray source to a detector was about 2 m and the samples were positioned in the midway. The beam angular divergence of $\sim$0.015° was accounted for in the data analysis. Specular reflectivity was obtained by subtraction of the background, which includes diffuse scattering, from the total intensity at the specular peak position.

3. Data Analysis and Results

X-ray specular reflectivity from the $\sim$290-Å-thick YBCO film on $SrTiO_3$ is shown in Fig. 1. A best fit (solid line) with a standard reflectivity model[30–33] shows three different layers, a disordered layer at top, a YBCO layer in the middle and a low density YBCO layer in the bottom as shown in the schematic diagram in the inset. The middle layer YBCO has thickness 205 ± 1 Å and roughness 12 ± 0.8 Å. We observed a layer of which the average electron density is $\sim$87% of a crystalline YBCO, with thickness 59 ± 2 Å and roughness 10.6 ± 0.6 Å between the substrate and the YBCO film. Since the electron density of the layer is higher than $SrTiO_3$ but lower than YBCO, we conclude that it is a low-density YBCO. This layer mostly contributes to the X-ray reflectivity in the region of the higher angle ($2\theta \geq 0.8°$) and diminishes the amplitude of the oscillation. This layer significantly improves the fit in higher angle region. Han *et al.*[27] have also observed this extra layer from a 2500-Å-thick YBCO film which was grown on a $SrTiO_3$ substrate by pulsed laser deposition. Although we do not know the origin of this layer, there are several possibilities. A remanent coating layer which was put to protect the surface of the $SrTiO_3$ substrate could cause the YBCO to have the low electron density, though the coating layer was completely removed before the deposition. A few monolayers deposited first possibly have different oxygen concentration, and intrinsic stress from the substrate might contribute to the deformation of the YBCO crystal. The X-ray reflectivity shows the existence of a disordered layer at the air/YBCO interface with thickness 27 ± 2 Å and roughness 5 ± 3 Å. The disordered layer might develop from oxidation at the air/YBCO interface. The X-ray scattering density of the disordered layer is about 11% of the crystalline YBCO. The roughness of the substrate was found to be $\sim$3 Å.

In order to understand the average crystalline structure of the YBCO film, X-ray diffraction measurements were carried out. Figure 2(a) shows the diffraction peaks along the substrate [001] direction. From the peak positions, the lattice constant *c* is found to be 11.69 ± 0.01 Å which corresponds to the oxygen concentration 6.96 per molecule ($x = 0.04$), and critical temperature $T_c \simeq 90$ K.[35] One third of the YBCO lattice constant is close to that of $SrTiO_3$. Because of limitations in the resolution, we were unable to discern between the supersymmetric diffraction peaks from the film and from the substrate. From a transverse scan (θ-rocking) at the YBCO (005) Bragg peak shown in the inset of (b), we found that the in-plane mosaicity of the YBCO film is about 0.5° which is one order of magnitude larger than that of the substrate. Figure 2(b) shows a plotting function for the width of the diffraction peak versus $\sin^2\theta$. As the domain size and residual strain broadening add as a

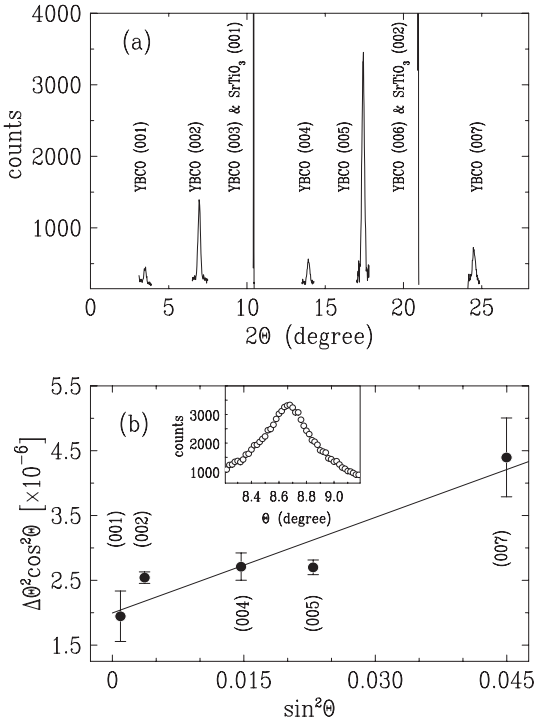

Fig. 2. (a) diffraction peaks from a YBCO/$SrTiO_3$ sample. (b) the broadenings of the diffraction peaks from the YBCO film in (a) versus θ, described in the text. The inset in (b) shows a transverse scan at the YBCO (005) peak.

Gaussian convolution, the plot is expected to be linear,[36] i.e.,

$$\Delta\theta^2 \cos^2\theta = \sin^2\theta\left(\frac{\Delta d}{d}\right)^2 + \left(\frac{\lambda}{L}\right)^2, \qquad (2)$$

where $\Delta\theta$ is the full width at half maximum of the diffraction peak, $\Delta d/d$ is the strain, λ is X-ray wavelength and L is the domain size. From a best fit (solid line), we found that the residual strain is $0.70 \pm 0.14\%$. This implies that the macroscopic compositional inhomogeneity within the film is negligible. The domain size was found to be 290 ± 70 Å, which can be compared to the total YBCO film thickness determined by GIXR.

Figure 3(a) shows the X-ray reflectivity from the Au/YBCO/$SrTiO_3$ sample. A best fit (solid line) shows that the roughness at the air/Au interface is 11.4 ± 0.1 Å and the thickness of Au film is 300.0 ± 0.3 Å. The disordered zone at the interface of Au/YBCO was found to be 7.6 ± 0.1 Å, which is about 2% of the YBCO film thickness (350 ± 1 Å). The YBCO thickness is close to 27 unit cells and the interdiffusion part is less than a single unit cell. We speculate that it is just the intrinsic YBCO surface roughness. In comparing the interface of Au/YBCO to the naked YBCO surface, we conclude that the gold film coated *in situ* on the YBCO film at room temperature protects the YBCO surface from degradation in air.

The X-ray reflectivity from the Ag/YBCO/$SrTiO_3$ sample is shown in (b). From the fit, the roughness at the interface, air/Ag, was found to be 10 ± 2 Å. The disordered zone at the Ag/YBCO interface, 15 ± 3 Å, can be comparable to that at the Au/YBCO interface. Winau *et al.*[38] have reported the observation of the interdiffusion of oxygen from YBCO into

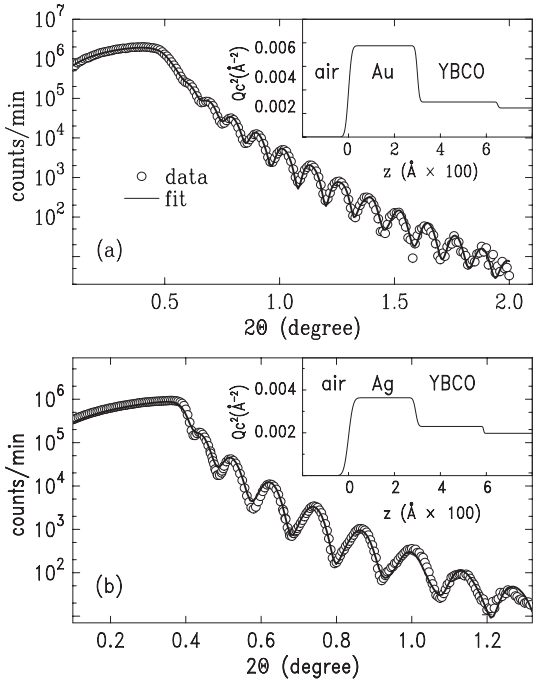

Fig. 3. Au/YBCO/$SrTiO_3$ (a) and Ag/YBCO/$SrTiO_3$ (b). The solid curve is a best fit and the inset shows the X-ray scattering density profile corresponding to the fit.

the Ag or Au coating layer at the substrate temperatures higher than 550°C. The temperature of our evaporation condition was room temperature and our results agree well with the observation of Winau *et al.*

Figure 4 shows the X-ray reflectivity from the Pb/YBCO/$SrTiO_3$ samples prepared *ex situ* (a) and *in situ* (b). It should be pointed out that we obtained the specular reflectivity by carefully subtracting the diffuse scattering part from the total intensity at specular reflection position in each transverse

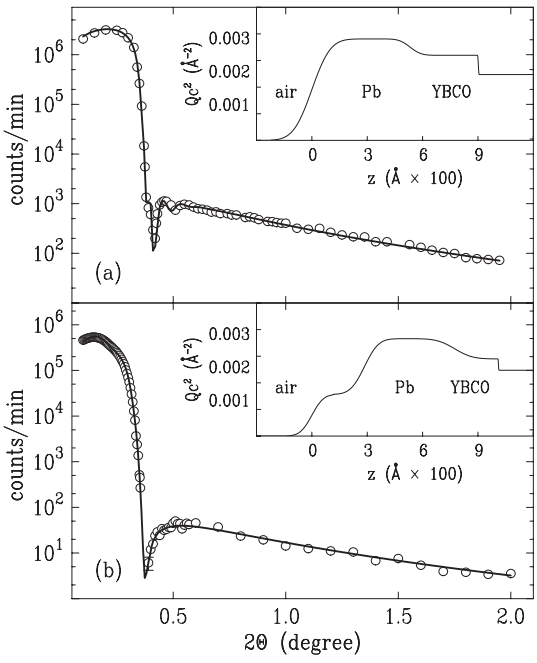

Fig. 4. Pb/YBCO/$SrTiO_3$ samples, Pb metalized *ex situ* (a) and *in situ* (b). The scattering density profiles corresponding to the fits (solid lines) are in the insets.

scan because the diffuse scattering was extremely strong near the critical angle and had a different scattering intensity profile in a transverse scan at each 2θ-position. The GIXR from Pb/YBCO is remarkably different from that from Au/YBCO or Ag/YBCO. Just above the critical angle, the reflectivity sharply drops down because of the huge surface roughness of the lead layer, the large X-ray absorption by the lead and the presence of a large disordered zone at the Pb/YBCO interface. At the high angles, the reflectivity is linear in a logarithmic scale, and is mainly determined by the smooth interface of the YBCO and substrate.

A best fit (solid line) to the reflectivity from the Pb/YBCO/$SrTiO_3$ sample prepared *ex situ* (a) shows interdiffusion at the Pb/YBCO interface 50 ± 10 Å and the roughness of Pb film 80 ± 10 Å. The scattering density of Pb is only 84% of the predicted value for a crystalline Pb, suggesting that the Pb film is entirely oxidized. A best fit to the X-ray reflectivity from the other Pb/YBCO/$SrTiO_3$ sample prepared *in situ* (b) shows that an oxide layer (thickness 285 ± 13 Å) developed on top of the Pb film and the Pb film itself is also completely oxidized. The interdiffusion at the Pb/YBCO interface is 75 ± 15 Å. The presence of a large disordered zone at the Pb/YBCO interface does not depend on whether the sample was grown *in situ* or *ex situ*. Although it is not clear where the oxygen in the Pb film comes from, it might come from air after the sample was taken out from the growth chamber since the lead film was grown under the pressure of 10^{-8} mTorr. However, some of the oxygen content could come from the YBCO film. We could not observe any diffraction peak from the Pb/YBCO film whereas the peaks up to YBCO (007) from the Au/YBCO and Ag/YBCO films were observed. This implies that the reaction between lead and YBCO destroys the YBCO crystalline structure.

4. Discussion

Development of a disordered layer at the air/YBCO interface can be a problem in fundamental research as well as practical applications. We have observed a disordered layer with thickness ~95 Å on the surface of a 6000-Å-thick YBCO film, as shown in Fig. 5. If we include the roughnesses at the interfaces, such as, air/disordered layer and disordered layer/YBCO, the effective thickness of the degradation layer is ~136 Å. Neutron reflectivity is quite similar to X-ray reflectivity. However the characteristics of neutrons are somewhat different from X-rays. Neutrons are less sensitive to small dead (oxide) layers at interfaces than X-rays because neutrons have a much smaller scattering and absorption cross section to oxygen than X-rays. The inset in Fig. 5 shows the neutron reflectivity from the YBCO film with the solid line a best fit. The fit yields a rms surface roughness of ~140 Å. A spin-polarized neutron reflectivity study by Han *et al.*[37] has shown that the roughness does not contribute to the surface magnetic screening length (London penetration depth) because the length is ~1400 Å, which is an order of magnitude larger than the roughness. However, the lower critical field (H_{c1}) of the film was ~4 times smaller than the predicted value for a smooth surface because the disordered zone at the surface reduces the Bean–Livingston surface barriers and helps early vortex entrance. It is not too surprising that a dead layer at the surface contributes to the surface effects. It should be emphasized that the disordered layer at the YBCO surface is a less superconducting layer rather than just a dead layer which is not a superconductor.

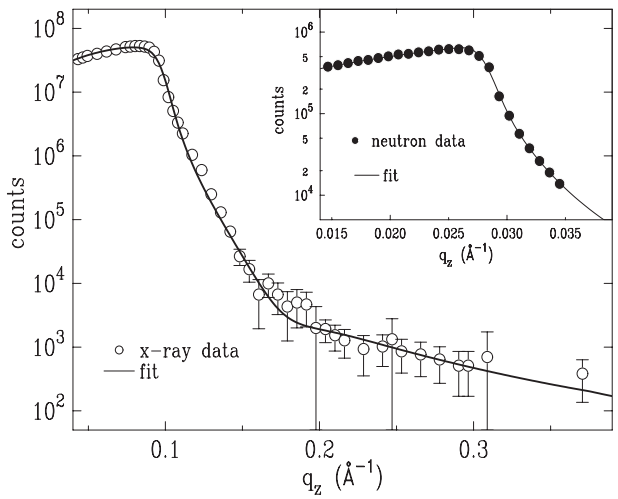

Fig. 5. X-ray and neutron (inset) reflectivities from a YBCO(6000 Å)/$SrTiO_3$ sample. The solid curve is a best fit.

Our X-ray diffraction measurements do not show diffraction peaks from the Au and Ag films which were grown on each YBCO(300 Å)/$SrTiO_3$. This implies that the gold and silver are amorphous. Because Au and Ag were deposited at room temperature, intrinsic stress between the gold (or silver) atoms and substrate[38] might effectively contribute to the deformation of a crystalline structure over the whole film. Moreover, Hasegawa *et al.*[39] have observed that the change of the surface morphology of Ag occurs at temperatures higher than 550°C. Because our growth temperature was much lower than the temperature for mobile Ag atoms, the Ag atoms might not have enough kinetic energy to move. We expect the same behavior with Au atoms. The interdiffusion at Au/YBCO and Ag/YBCO interfaces, which is about one unit cell, agrees well with a smallest value of the YBCO surface roughness with the stoichiometry (1 : 2 : 3 within 1–2% uncertainty) accurately controlled during coevaporation.[6] We should point out that different deposition techniques were used for preparing the YBCO films underneath Au and Ag; namely, they were grown by magnetron sputtering and coevaporation, respectively. Our observation of a small disordered zone at the interfaces of Au/YBCO and Ag/YBCO agrees with previous studies.[23–25,38]

Independent of the growth conditions, *in situ* and *ex situ*, the interdiffusion at the Pb/YBCO interface was about 60 Å. Although the large disordered interfacial region at air/Pb and the oxidation over the whole lead film could occur after the samples were exposed to air, the interdiffusion at Pb/YBCO interface may exist already in the growth chamber. Since the interdiffusion was determined by rms roughness, the effective interdiffusion zone could be larger than 60 Å. It is very surprising that Lesueur *et al.*[6] observed a similar Josephson current across both *in situ* YBCO/Pb and *in situ* YBCO/Ag/Pb planar tunnel junctions. They used about 100-Å-thick Ag layer in-between YBCO and Pb. The disordered zone at the Pb/YBCO interface might play a similar role as the Ag layer. From X-ray reflectivity studies, it is not clear

whether the oxygen concentration in the YBCO film is changed due to the reaction between Pb and YBCO, and also whether the lead atoms are likely to bond with particular types of atoms in YBCO. The study of local structure around the Pb atoms in the disordered zone of the Pb/YBCO interface, *in situ* glancing incident X-ray absorption fine structure study for example, could reveal the environment of the Pb atoms and the reaction between the lead and the YBCO.

5. Conclusions

By using GIXR, which is a microscopical probe with a resolution of a single atomic size, we studied laterally averaged surfaces and interfaces of a high-T_c superconductor and metals. The metal films (Au, Ag and Pb) were deposited on YBCO near room temperature, *in situ* and *ex situ*. The reaction between Pb and YBCO created large interdiffusion, ~50–80 Å, at their interface and destroyed the crystalline structure of the 300-Å-thick YBCO film. A large degradation zone at the Pb surface which was exposed to air was observed and the lead layer was entirely oxidized. The interfaces of Au/YBCO and Ag/YBCO remained clean. This suggests that the gold and silver films electronically contact YBCO well. From the 300-Å-thick and 6000-Å-thick YBCO films, we observe a disordered layer at the air/YBCO interface and the disordered zone is extended with the YBCO film thickness.

Acknowledgments

Support of works at University of Missouri is gratefully acknowledged from the Midwest Superconductivity Consortium (MISCON) under DOE grant DE-FG02-90ER45427 and the NSF DMR 96-23827, work at University of Illinois was done under auspices of the NSF DMR 94-21957 and ONR N-00014-95-1-0831.

1) G. B. Lubkin: Phys. Today (Mar., 1996) 48.
2) G. Blatter, M. V. Feigel'man, V. B. Geshkenbein, A. I. Larkin and V. M. Vinokur: Rev. Mod. Phys. **66** (1994) 1125.
3) M. Covington, R. Scheuerer, K. Bloom and L. H. Greene: Appl. Phys. Lett. **68** (1996) 1717.
4) M. Aprili, M. Covington, E. Paraoanu, B. Niedermeier and L. H. Greene: Phys. Rev. B **57** (1998) 8139.
5) A. S. Katz, A. G. Sun, R. C. Dynes and K. Char: Appl. Phys. Lett. **66** (1995) 105.
6) J. Lesueur, M. Aprili, A. Goulon, T. J. Horton and L. Dumoulin: Phys. Rev. B **55** (1997) 3398.
7) D. F. Agterberg and M. Sigrist: Phys. Rev. Lett. **80** (1998) 2689.
8) K. A. Kouznetsov, A. G. Sun, B. Chen, A. S. Katz, S. R. Bahcall, J. Clarke, R. C. Dynes, R. A. Gajewski, S. H. Han, M. B. Maple, J. Gianpintzakis, J.-T. Kim and D. M. Ginsberg: Phys. Rev. Lett. **79** (1997) 3050.
9) R. Kleiner, A. S. Katz, A. G. Sun, R. Summer, D. A. Gajewski, S. H. Han, S. I. Woods, E. Dantsker, B. Chen, K. Char, M. B. Maple, R. C. Dynes and J. Clarke: Phys. Rev. Lett. **76** (1996) 2161.
10) D. A. Wollman, D. J. Van Harlingen, J. Giapintzakis and D. M. Ginsberg: Phys. Rev. Lett. **74** (1995) 797.
11) I. Iguchi and Z. Wen: Phys. Rev. B **49** (1994) 12388.
12) J. H. Xu, J. L. Shen, J. H. Miller, Jr. and C. S. Ting: Phys. Rev. Lett. **73** (1994) 2492.
13) J. C. Macfarlane, L. Hao, D. A. Peden and J. C. Gallop: Appl. Phys. Lett. **76** (2000) 1752.
14) D. S. Dessau, B. O. Wells, Z.-X. Shen, W. E. Spicer, A. J. Arko, R. S. List, C. G. Olson, C. B. Eom, D. B. Mitzi, A. Kapitulnik and T. H. Geballe: Appl. Phys. Lett. **58** (1991) 1332.
15) P. V. Komissinski, E. Il'ichev, G. A. Ovsyannikov, S. A. Kovtonyuk, M. Grajcar, R. Hlubina, Z. Ivanov, Y. Tanaka, N. Yoshida and S. Kashiwaya: cond-mat/0106559.
16) W. Wang, M. Yamazaki, K. Lee and I. Iguchi: Phys. Rev. B **60** (1999) 4272.
17) R. P. Robertazzi, A. W. Kleinsasser, R. B. Laibowitz, R. H. Koch and K. G. Stawiasz: Phys. Rev. B **46** (1992) 8456.
18) R. Kalyanaraman, S. Oktyabrsky and J. Narayan: J. Appl. Phys. **85** (1999) 6636.
19) R. Singh, D. Bhattacharya, P. Tiwari, J. Narayan and C. B. Lee: Appl. Phys. Lett. **60** (1992) 255.
20) D. Kumar, M. Sharon, R. Pinto, P. R. Apte, S. P. Pai, S. C. Punandare, L. G. Gupts and R. Vijayaraghaven: Appl. Phys. Lett. **62** (1993) 3522.
21) R. Pinto, P. R. Apte, M. S. R. Rao, Ramesh Chandra, C. P. Pai, L. C. Gupta, R. Vijayaraghavan, K. I. Gnanasekar and M. Sharon: Appl. Phys. Lett. **68** (1996) 1006.
22) M. Z. Cieplak, G. Xiao, C. L. Chien, A. Bakhshai, D. Artymowicz, W. Bryden, J. K. Stalick and J. J. Rhyne: Phys. Rev. B **42** (1990) 6200.
23) Z. H. Gong, F. Vassenden, R. Fagerberg, J. K. Grepstad, A. Bardal and R. Hoier: Appl. Phys. Lett. **63** (1993) 836.
24) S.-W. Chan, L. Zhao, X. Chen, Q. Li and D. B. Fenner: J. Mater. Res. **10** (1995) 2428.
25) Q. Y. Ma, M. T. Schmidt, E. S. Yang, Siu-Wai Chan, D. Bhattachayra, J. P. Zheng and H. S. Kwok: J. Appl. Phys. **71** (1992) 4082.
26) A. G. Zaitsev, R. Schneider, J. Geerk, G. Linker, F. Ratzel and R. Smithey: Appl. Phys. Lett. **75** (1999) 4165.
27) S.-W. Han, J. A. Pitney, P. F. Miceli, M. Covington, L. H. Greene, M. J. Godbole and D. H. Lowndes: Physica B **221** (1996) 235.
28) W. J. Lin, P. D. Hatton, F. Baudenbacher and J. Santiso: Physica B **248** (1998) 56.
29) T.-S. Gau, S.-L. Chang, H.-H. Hung, C.-H. Lee, T.-W. Huang, H.-B. Lu, S.-J. Yang and S.-E. Hus: Appl. Phys. Lett. **65** (1994) 1720.
30) S. K. Sinha, E. B. Sirota, S. Garoff and H. B. Stanley: Phys. Rev. B **38** (1988) 2297.
31) T. P. Russell: Mater. Sci. Rep. **5** (1990) 171.
32) P. F. Miceli: *Semiconductor Interfaces, Microstructures and Devices: Properties and Applications*, ed. Z. C. Feng (IOP Publishing, Bristol, 1993) p. 87.
33) L. G. Parratt: Phys. Rev. **95** (1954) 359.
34) L. H. Greene, B. G. Bagley, W. L. Feldman, J. B. Barner, F. Shokoohi, P. F. Miceli, B. J. Wilkins, V. Pendrick, D. Kalokitis and A. Fathy: Appl. Phys. Lett. **59** (1991) 1629.
35) D. C. Johnston, A. J. Jacobsen, J. M. Newsam, J. T. Lewndowski, D. P. Goshorn, D. Xie and W. B. Yelon: in *Chemistry of High Temperature Superconductors*, eds. D. L. Nelson, M. S. Wittingham and T. F. George (American Chemical Society, Washington, D.C., 1987) p. 136.
36) P. F. Miceli, T. Venkatesan, X. D. Wu and J. A. Potenza: AIP Conf. Proc. **165** (1988) 150.
37) S.-W. Han, J. F. Ankner, H. Kaiser, P. F. Miceli, E. Paraoanu and L. H. Greene: Phys. Rev. B **59** (1999) 14692.
38) D. Winau, R. Koch, M. Weber, K.-H. Rieder, R. K. Garg, T. Schurig and H. Koch: Appl. Phys. Lett. **61** (1992) 279.
39) M. Hasegawa, Y. Yoshida, M. Iwata, H. Akata, K. Higashiyama, Y. Takai and I. Hirabayashi: Jpn. J. Appl. Phys. **39** (2000) 1719.